Currents in defective coupled ratchets

A. J. Fendrik and L. Romanelli*
Instituto de Ciencias, Universidad Nacional de General Sarmiento–J.M. Gutierrez 1150, (1613) Los Polvorines, Buenos Aires, Argentina and Consejo Nacional de Investigaciones Científicas y Técnicas–Buenos Aires, Argentina

M. V. Reale
Instituto de Ciencias, Universidad Nacional de General Sarmiento–J.M. Gutierrez 1150, (1613) Los Polvorines, Buenos Aires, Argentina
(Received 4 January 2012; revised manuscript received 20 March 2012; published 27 April 2012)

Transport phenomena in a one-dimensional system of interacting particles is studied. This system is embedded in a periodic and left-right asymmetric potential driven by a force periodic in time and space. When the density (number of particles per site) is an integer, directional current of the particles is collective; that is, it involves the whole system since all the sites are equivalents. On the other hand, when the system has a defect, a new localized or noncollective current appears due to the migration of defects from one site to another. We show here how this "defective" (defects generated) current can be controlled by white noise.

DOI: 10.1103/PhysRevE.85.041149 PACS number(s): 05.40.−a, 05.60.−k, 05.10.Gg

I. INTRODUCTION

A ratchet system consists of a set of particles far from equilibrium that may show a directional current, even though the acting forces have zero mean value (see the comprehensive reviews [1] and [2]). The particles may be interacting or not. These systems can be classified as deterministic [3], stochastic [4] (Brownian), and inertial [5,6] (underdamped) or overdamped and have the peculiarities to present different regimes, so that the variation of some parameters can generate, for instance, a current reversal. Since the first pioneering works [7,8], ratchets have become an object of interest in many fields [9], as they provide models for transport in biological systems [10–13] and inspire the design and construction of (classical or quantum) artificial devices [14] (and references therein).

In this work, we analyze the dynamics of a deterministic coupled ratchet, the same as in Ref. [15], but with a novelty: The number of particles here is not a multiple of the number of minima of the ratchet potential; that is, the density, the number of particles per site, can be a rational number. In previous papers where the density was an integer, the configurations were equivalent to perfect lattices and the transport effects were collective and extended phenomena. Here, with noninteger densities the system will have some kind of disorder (broken symmetries) and as a consequence a new noncollective localized transport regime associated with the migration of defects will appear. We remark that this type of disorder is quite different from the one described in Ref. [16], where defects were introduced in the ratchet potential, and it is not comparable to the punctual defects (interstitials or vacancies) that can occur in perfect lattices. The defective configurations to consider generate metastable states in infinite arrays [17] and become equilibrium states when periodic boundary conditions are imposed. The system is based in an overdamped, driven Frenkel-Kontorova model [18] that is widely used to describe phenomena such as dislocations, Josephson junction arrays [19–21], proton transport in biological molecules and icelike crystals [22], nonlinear DNA dynamics [23], tribology, interfacial slip and microscopic models of friction (nanotribology) [24], and models for collective ratchets [25–27].

In previous papers [5,15,28], we showed that with integer densities, the system has different regimes in different regions of parameters space. The relevant parameters were density (always an integer), coupling constant, and external force. The different regimes were characterized by different orbits corresponding to different behavior, for instance, the flow direction changed across the boundary between two regions in parameters space. We also showed that a moderate amount of noncorrelated noise induces regime transitions. For instance, choosing adequate parameters, white noise caused an inversion in the current direction.

The paper is organized as follows: In the following section, a description of the model is given; Sec. III is devoted to determining the possible currents of the stationary orbits according to the density of particles regardless of the interaction and the shape of the ratchet potential. In Sec. IV we determine the regions in the parameter space where these currents occur. The effect of white Gaussian noise is discussed in Sec. V, and finally, in the last section, the conclusions are drawn. The Appendix is devoted to showing the dimensionless equation of motion.

II. THE MODEL

The system under study consists of N interacting particles placed in a one-dimensional ring of length L subject to a periodic potential $V_\alpha(x)$ and driven by an external force in the overdamped regime.

The time evolution of the ith particle is given by the equation

$$\eta\dot{x}_i(t) + \frac{\partial V_\alpha(x_i)}{\partial x_i} + \frac{\partial V^{\rm osc}(x_{i-1},x_i,x_{i+1})}{\partial x_i} = F^{\rm dr}(x_i,t) + \sigma\,\xi_i(t). \quad (1)$$

In Eq. (1), $x_i(t)$ represents the coordinate of the ith particle, $i = 1,2,\ldots,N$ with the conventions $x_{N+1} = x_1$ and $x_0 = x_N$.

*lili@ungs.edu.ar

These are measured in the counterclockwise direction along a ring of length L, therefore fulfilling the periodicity condition $x_{i+L} = x_i$. $V_\alpha(x)$ is a one-dimensional, left-right asymmetric periodic potential defined by

$$V_\alpha(x) = \begin{cases} V_o\left(\cos\left[\frac{\pi}{\alpha}\left(\frac{(\alpha+1)x}{d}\right)\right]\right), & \text{for } 0 \leqslant \frac{x}{d} \leqslant \frac{\alpha}{(\alpha+1)} \\ -V_o\left(\cos\left\{\pi\left[(\alpha+1)\frac{x}{d} - \alpha\right]\right\}\right), & \text{for } \frac{\alpha}{(\alpha+1)} \leqslant \frac{x}{d} \leqslant 1 \end{cases} \tag{2}$$

and the periodicity constraint $V_\alpha(x+d) = V_\alpha(x)$ outside the interval $(0,d)$. Thus, the total length of the circle is $L = sd$, where s is the number (even) of minima and d is the linear distance between consecutive minima of the ratchet. α ($\alpha > 0$) controls the left-right asymmetry. Solutions for $\alpha > 1$ in which the minima of the wells of the ratchet are displaced in the counterclockwise direction are equal to the time-reversed solutions, with $\alpha < 1$ in which the minima are displaced in the opposite (clockwise) direction.

The coupling potential is

$$V^{\text{osc}}(x_{i-1}, x_i, x_{i+1}) = \tfrac{1}{2}k[(x_{i-1} - x_i)^2 + (x_i - x_{i+1})^2]. \tag{3}$$

In addition, the particles are driven by an external periodic force $F^{\text{dr}}(x_i,t)$ given by the gradient of a time-dependent potential with a spatial periodicity that is twice that of V_α:

$$F^{\text{dr}}(x_i,t) = -\varepsilon\frac{\partial V^{\text{dr}}(x_i,t)}{\partial x_i} = -\varepsilon\sin(\omega t)\frac{\partial \sin(\pi x_i/d)}{\partial x_i}. \tag{4}$$

With this choice, consecutive wells alternate in time as absolute minima. The driving is a longitudinal standing wave over the ring. If the applied force is only Eq. (4), that is without the static ratchet potential Eq. (2) and without interactions, then in the overdamped regime, the particles oscillate around their initial position.

The last term in Eq. (1) represents a Gaussian white noise source satisfying the condition $\langle \xi_i(t)\xi_i(t')\rangle = \delta(t-t')$. The factor σ is equal to $\sqrt{2k_BT}$ (where k_B is the Boltzmann constant) so that the last term in the equation corresponds to a thermal bath of temperature T.

We solve the dimensionless Eq. (1) (as described in the Appendix). We define four dimensionless quantities, $\Pi_k = k(sd/N)^2/2V_o$, $\Pi_\varepsilon = \varepsilon/2V_o$, $\Pi_T = k_BT/2V_o$, and $\Pi_\eta = (\eta d^2)/(2V_o\tau)$, where N is the number of particles and $\tau = 2\pi/\omega$ is the period of driving force Eq. (4). Π_k is a measure of the average potential elastic energy per particle in units of the depth of the periodic potential. The parameter Π_ε compares the energy provided by the external driving with the depth of the ratchet potential $2V_o$. The parameter Π_T compares the energy delivered by the thermal bath also with the depth of the ratchet potential. The last parameter Π_η compares the average energy dissipated by the damping force with the depth of the ratchet potential. All the calculations that we report were made for $\Pi_\eta = 1$ and $\alpha = 1/3$. The space spanned by the other parameters (mainly the strength interaction k, the amplitude ε and the temperature T) is explored in order to have a general picture of the dynamics of the system. We consider that the particles cannot interpenetrate, i.e., they preserve their relative order in the ring. This fact introduces elastic collisions that can be taken into account by renaming the particles wherever they intersect. For identical particles, an elastic collision is an exchange of velocities.

In Fig. 1 we show the effect of the driving. According to the values of the parameters Π_k, Π_ε, the particles can move backward [Fig. 1(a)] or forward [Fig. 1(b)]. In addition, Fig. 2 shows the position of the eight particles as a function of time

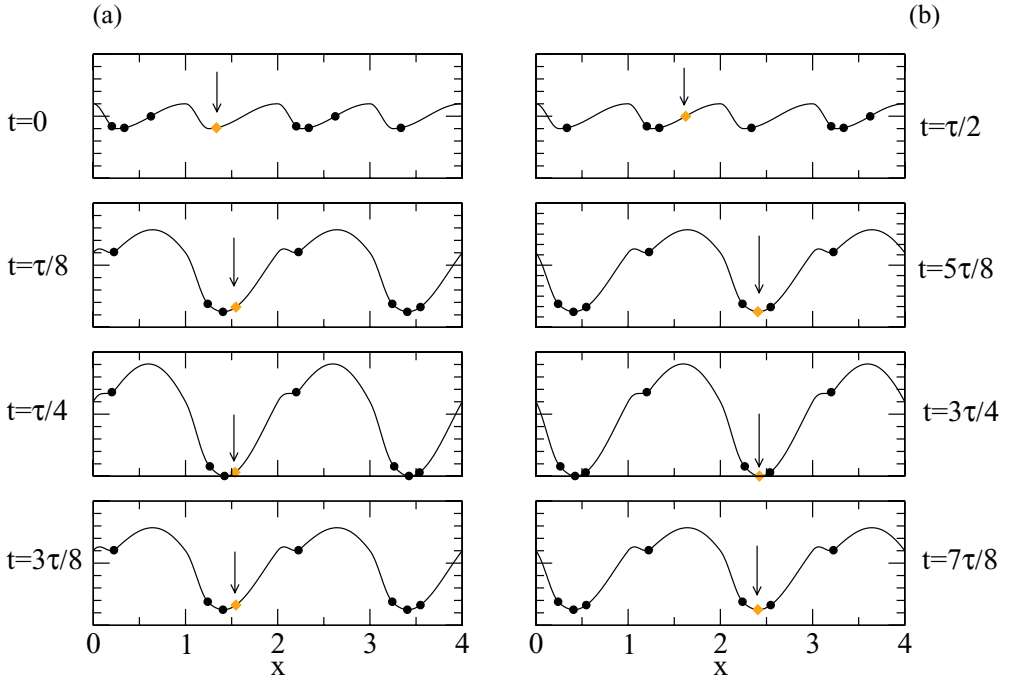

FIG. 1. (Color online) Position x on the ring for $N = 8$ particles and total potential $V(x,t) = V_\alpha(x) + \epsilon V^{\text{dr}}(x,t)$. We have marked a particle [light gray (orange)] with an arrow to display its evolution. The parameters Π_k and Π_ε correspond to velocities (a) $\bar{v} < 0$ and (b) $\bar{v} > 0$.

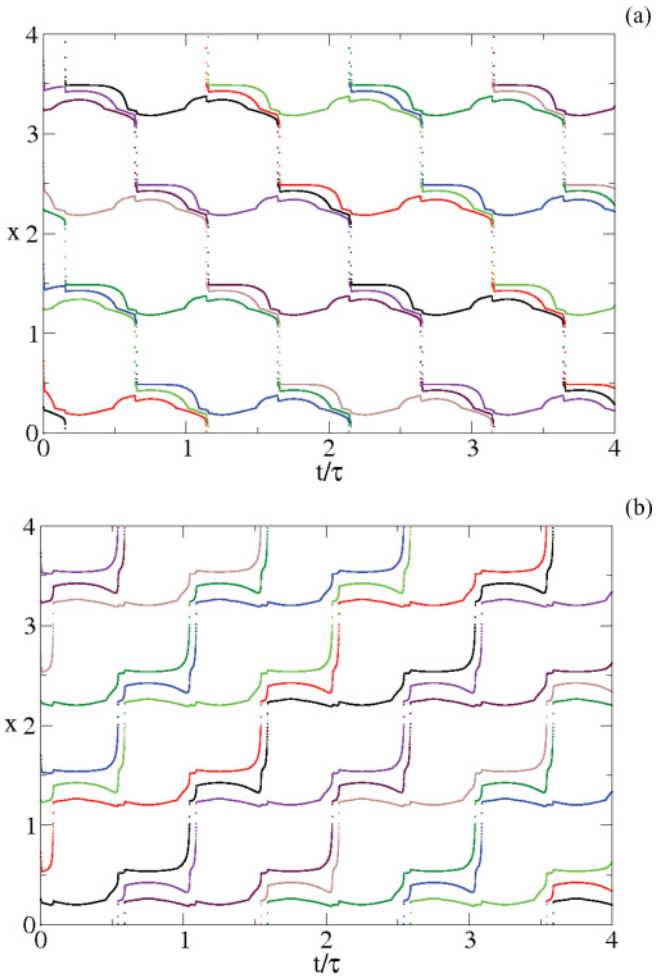

FIG. 2. (Color online) Time evolution for $N = 8$. The position on the ring x for each particle as a function of time t. (a) and (b) correspond to the parameters Π_k and Π_ε of Figs. 1(a) and 1(b), respectively.

corresponding to cases (a) and (b) shown in Fig. 1. Time here runs from the start to $t = 4\tau$, allowing us to verify that the system reaches the steady state very quickly.

III. THE POSSIBLE CURRENTS

In this section we show how the continuity constraint (conservation of the number of particles) and the symmetries in time and space of the potentials characterize the possible stationary currents.

The velocity is defined by

$$\bar{v} = s \lim_{n_o \to \infty} \frac{n_w(n_o)}{n_o}, \tag{5}$$

where s is the number of sites and $n_w(n_o)$ is the number of turns around the ring after n_o oscillations of the driving force Eq. (4). The particle current will be

$$\bar{j} = \bar{v}\rho, \tag{6}$$

where N is the number of particles and $\rho = N/s$ is the density of particles.

In the present work, we will restrict our discussion to defective systems where there is only one extra particle in one site (see Fig. 3). In other words, $N = (sl) + 1$, where l is an integer and therefore ρ is not an integer.

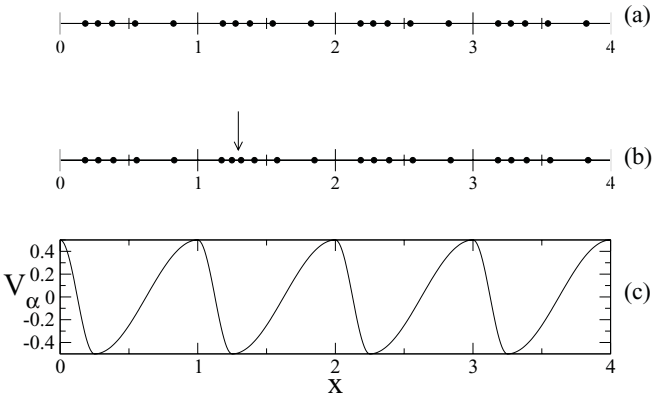

FIG. 3. When the density ρ is an integer [panel (a), $\rho = 5$], the static equilibrium configuration ($\Pi_\varepsilon = 0$) shows an equal number of particles per site (perfect lattice). When ρ is not an integer, the configuration is defective [panel (b), $\rho = 5.25$]. The arrow indicates an extra particle in the second site (an interstitial). In panel (c), the static (ratchet) potential, with $\alpha = 1/3$, is plotted.

To simplify the description we imagine the ratchet potential deep enough so that most of the time the particles lie at the bottom of the potential—the sites—and the dynamics reduces to transitions between "states," which are fully described by giving the number of particles lying in each site. All potentials are invariant under translation in twice the intersite distance, and the external potential is also invariant under time translations in one period. We assume that the stationary dynamics has the maximum residual symmetry.

In order to distinguish and classify the dynamics we now imagine taking an instantaneous picture at each half-period in time exactly when the external potential is in phase with the ratchet potential. Then from the symmetry arguments it follows that the occupation number distribution along sites will be $n,m,n,m,n,m \ldots n,m$ for the nondefect ratchet, while in the defective one with one excess or missing particle the distribution will only differ in one site where the (plus or minus) defect sits as, for instance, $n,m,n+1,m,n,m \ldots n,m$. In the next half-period, the occupation number distribution will be $m,n,m,n,m,n \ldots m,n$ for the perfect ratchet, and for the defective one there are two cases: (a) If the defect remains in the same site, $m,n,m+1,n,m,n \ldots m,n$. (b) If the defect migrates $m,n+1,m,n,m,n \ldots m,n$ or $m,n,m,n+1,m,n \ldots m,n$.

To derive the particle currents we finally argue that as a consequence of the overdamping assumptions in each half-period particles will migrate from sites where the external potential is maximum toward sites where it is minimum (this will not necessarily be the case if inertia was important). Therefore, if $n > m$ a fraction r of the $n - m$ particles will migrate to the left and $n - m - r$ will go to the right, so that the net flux of particles ϕ_p across all but one intersite separation in a full period will be

$$\phi_p = n - m - 2r \tag{7}$$

with $r \leqslant n - m$ so that $-(n - m) \leqslant \phi_p \leqslant n - m$. The defect can also move to the adjacent site adding 1 (or -1 if it is a hole) to the flux in that particular intersite. So finally the

mean current per period for a ratchet with s sites will take the possible values

$$\bar{j} = -p, -p+2, \ldots, 0, 2, \ldots p-2, p, \tag{8}$$

where $p = n - m$ for perfect ratchet or if the defect does not migrate, or $p = n - m \pm 2/s$ if the defect migrates. Therefore, the total current will have two contributions $\bar{j} = \bar{j}_c + \bar{j}_d$. The collective current ($\bar{j}_c = l$ integer) and that due to the migration of the defect ($\bar{j}_d = \pm 2/s$) so that the velocities are $|\bar{v}| = |l \pm 2/s|(s/N)$. When the current is only due to the migration of the defect $l = 0$, $\bar{j} = \pm 2/s$ and $\bar{v} = \pm 2/N$. In such a case, there is an alternative way to determine the current. Since the defect has $\bar{v_d} = \pm 2$ and $\rho_d = 1/s$, it the turns out that $\bar{j}_d = \pm 2/s$.

Consequently, this analysis allows us to establish a necessary but not sufficient condition that the currents must satisfy. These arguments apply regardless of the interaction and the particular shape of the ratchet potential.

IV. STATIONARY ORBITS AND THEIR CURRENTS

In a previous paper [15], we found the separatrices and the phase diagram in the plane $(\Pi_k - \Pi_\varepsilon)$ for $\rho = 2$ without noise. It is displayed in Fig. 4(a) for $N = 8$ particles in $s = 4$ wells. The regions are labeled with the values of $\bar{v}$ of the corresponding stationary orbit and the numbers on each region indicate the mean velocity $\bar{v}$. The corresponding currents are

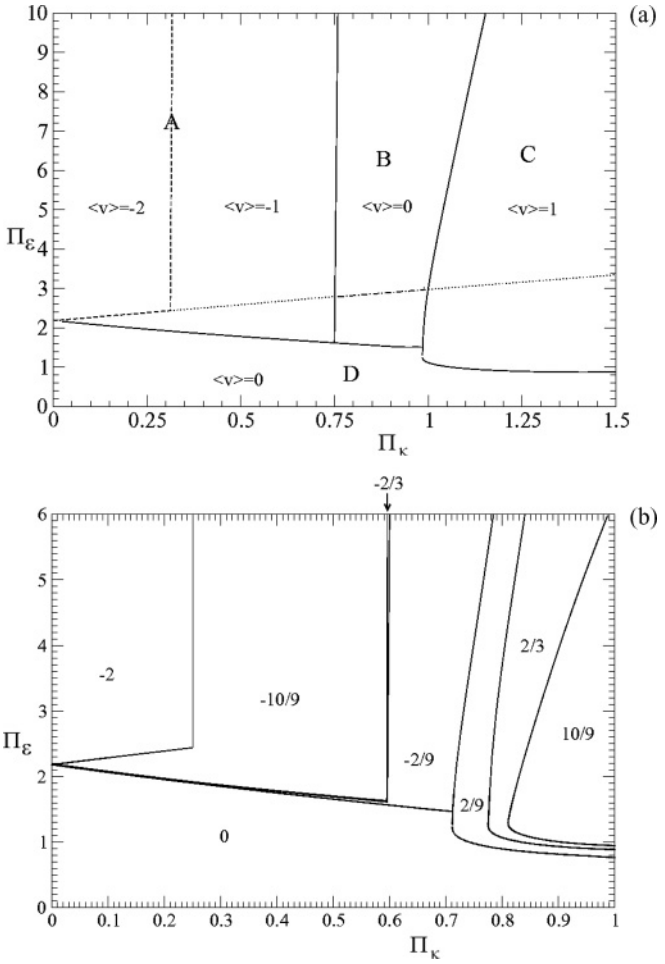

FIG. 4. (a) Phase diagram of the dynamics in the plane Π_k vs Π_ε for $\Pi_T = 0$ and $\rho = 2$ from Ref. [15]. (b) Phase diagram of the dynamics in the plane Π_k vs Π_ε for $\Pi_T = 0$ and $\rho = 9/4$.

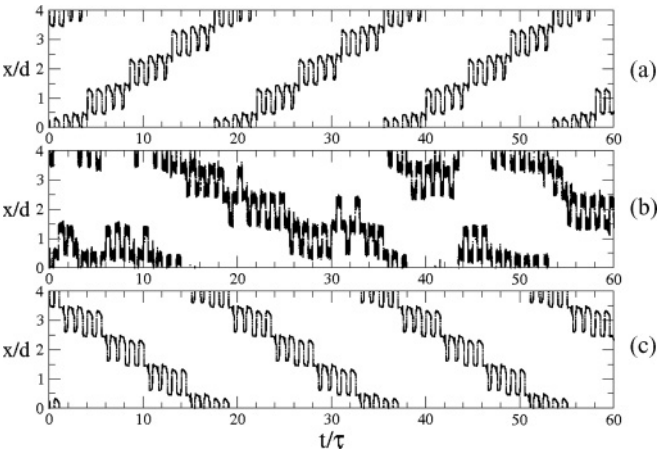

FIG. 5. Time evolution for $N = 9$, $s = 4$, (a) deterministic orbit, $\Pi_T = 0$, $\Pi_k = 0.7348$, $\Pi_\varepsilon = 3.0$, $\bar{v} = 2/9$; (b) noisy orbit $\Pi_T = 0.15$, $\Pi_k = 0.7348$, $\Pi_\varepsilon = 3.0$; (c) deterministic orbit $\Pi_T = 0$ $\Pi_k = 0.7348$, $\Pi_\varepsilon = 3.35$, $\bar{v} = -2/9$. By adding white Gaussian noise to (a) we obtain (b), which reproduces (c), inverting the current.

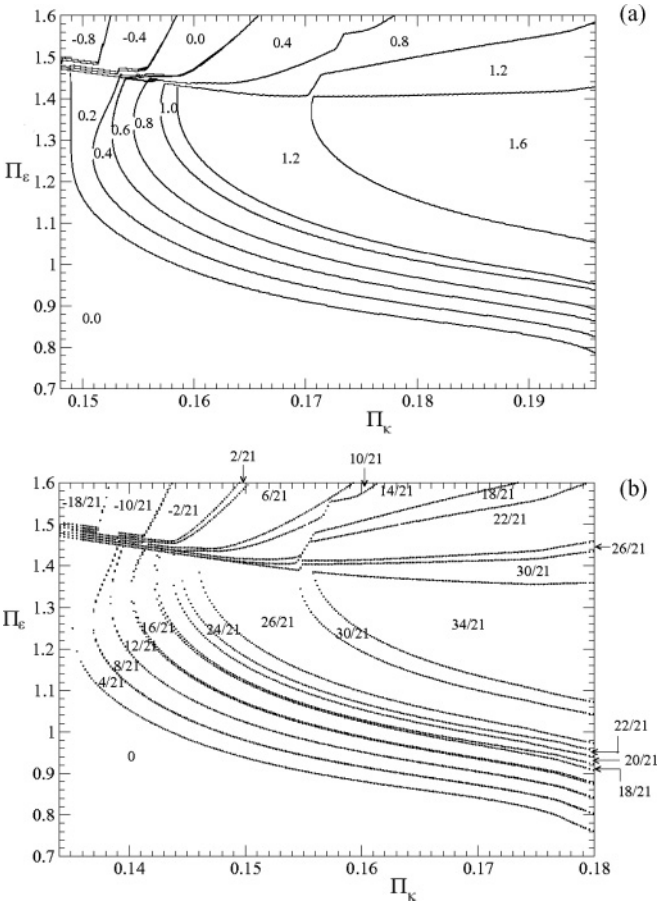

FIG. 6. (a) Phase diagram of the dynamics in the plane Π_k vs Π_ε for $\Pi_T = 0$ and $\rho = 5$ from Ref. [28]. (b) Phase diagram of the dynamics in the plane Π_k vs Π_ε for $\Pi_T = 0$ and $\rho = 21/4$.

collective and take the values $0, \pm 2$, and 4. The regions that correspond to velocities in opposite directions are separated by regions of null velocity.

By adding a particle to the system, the corresponding diagram is shown in Fig. 4(b) ($N = 9$ and $s = 4$). The values of the currents in each region are $0, \pm 0.5, \pm 1.5, \pm 2.5, 4.5$. The values ($\pm 0.5$) correspond to transport provided by just the migration of the defect while the others have an additional collective contribution.

The region in which the perfect system ($N = 8, s = 4$) had zero mean velocity is split now in regions with different speeds; in particular, the two contiguous regions ($\bar{v} = 2/9, \bar{v} = -2/9$) are due to the defect migrating. The orbit characteristics (for a particle) in both regions are shown in Figs. 5(a) and 5(c), respectively.

A similar phenomena is observed if a particle is removed. In this case, the current is provided by the vacancy migration in the opposite direction of the particles.

We also analyzed the cases for $N = 20$ [28] and $N = 21$, observing the same phenomenon. Here the parameters Π_ε and Π_k are chosen close to their values for $N = 20$ where the speed was zero [see Fig. 6(a)], and we can see the regions of collective currents $0, 1, \pm 2, 3, \pm 4, 5, 6$, and 8. The diagram for $N = 21$ is displayed in Fig. 6(b). There are pure collective currents (1,2,3,4,5,6), currents having collective and defective contribution (1.5, ± 2.5,3,5, ± 4.5,5.5,6.5,7.5,8.5), and the regions $\bar{j} = \bar{j}_d = \pm 0.5$ that correspond to pure defect migration. The latter, again, appear where the system $N = 20$ showed a region with zero current.

V. THE EFFECT OF NOISE

In this section we study the effect of adding white Gaussian noise to a defective system in parameter space such that there are no collective currents (i.e., the parameters correspond to $j_c = 0$). For $N = 9$, the orbits shown in Figs. 5(a) and 5(c) belong to systems whose parameters Π_ε and Π_k correspond to the regions of $\bar{v} = \pm 2/9$, respectively. The addition of Gaussian white noise to the system maintaining the values of the parameters unchanged causes a reversion in the direction of the current as can be seen in Figs. 5(a) and 5(b).

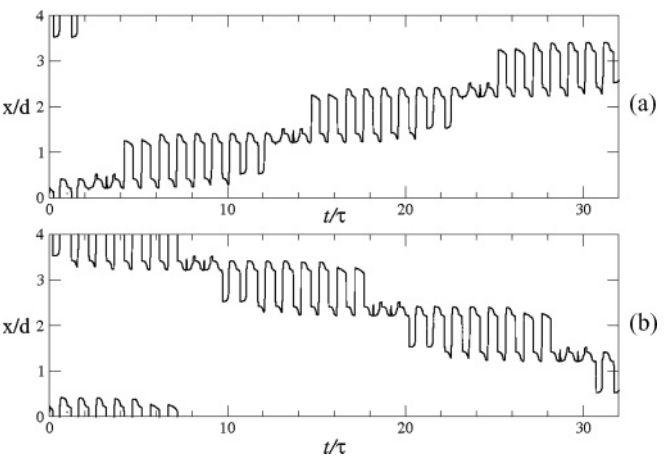

FIG. 7. Time evolution for $N = 21, s = 4$. (a) Deterministic orbit $\Pi_T = 0$, $\Pi_k = 0.1487$, $\Pi_\varepsilon = 1.561$, $\bar{v} = 2/21$; (b) deterministic orbit $\Pi_T = 0$, $\Pi_k = 0.1487$, $\Pi_\varepsilon = 1.59$, $\bar{v} = -2/21$.

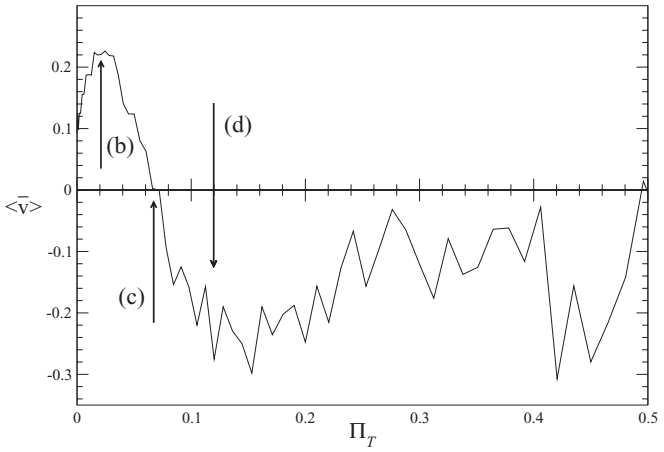

FIG. 8. Time evolution for $N = 21$, $s = 4$. Average mean velocity $\bar{v}$ vs noise intensity Π_T for the parameters $\Pi_k = 0.1487$ and $\Pi_\varepsilon = 1.561$. The arrows [labeled by (b), (c), and (d)] indicate the values of noise corresponding to the typical orbits displayed in Figs. 9(b)–9(d), respectively.

Similar effects are observed for $N = 21$. Figures 7(a) and 7(b) display the deterministic orbits for $\bar{v} = \pm 2/21$. With the parameters $\Pi_k = 0.1487$ and $\Pi_\varepsilon = 1.561$ fixed, $\bar{v} = 2/21$ [Fig. 9(a)] and the addition of noise to the system generates different velocities. Figure 8 shows the velocity $\langle \bar{v} \rangle$ of the particles as a function of the noise. The bracket indicates a mean value of over 20 realizations. Here we see that initially (for low noise) the velocity increases, reaches a maximum and then decreases, passes through zero, and then reverses. The noisy trajectories shown in Fig. 9 correspond to the noise values indicated by the arrows in Fig. 8.

This behavior in the presence of a moderate level of noise is related to what happens in stochastic resonators and stochastic ratchets. While the deterministic dynamics is in general robust against added noise, this can still induce transitions between

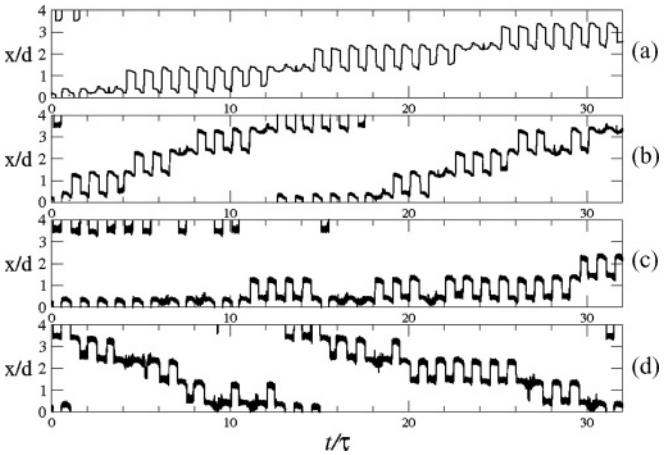

FIG. 9. Position on the ring of one particle as a function of t/τ for $N = 21$, $s = 4$. (a) The orbit for the deterministic system $\Pi_T = 0$. (b) Typical orbit corresponding to the maximum ($\Pi_T = 0.02048$). (c) Typical orbit $\bar{v} = 0$ ($\Pi_T = 0.068445$). (d) Typical orbit for which the noise induces a current inversion ($\Pi_T = 0.120125$).

the different stationary trajectories of the deterministic system. In the case of stochastic resonance, a bistable system perturbed by a monochromatic force, the deterministic system has two types of paths: small-amplitude librations around each of the minimum and beyond a certain value of the disturbance, high-amplitude librations between the minima. The addition of an optimal noise in conditions of small-amplitude librations leads to the dynamics of large- amplitude librations. In the case of stochastic ratchets, the deterministic system presents both small-amplitude librations and a directional rotation depending on the values of the parameters. Noise added to the system in libration conditions produces a transition to directional rotation. In the defective ratchet system with $N = 9$, the addition of noise to the deterministic system with $\bar{j} = \bar{j}_d$ induces a transition to stationary trajectory with $\bar{j} = -\bar{j}_d$. This can be seen clearly in Fig. 5. For $N = 21$, transitions caused by noise are not restricted to the stationary orbit with $\bar{j} = -\bar{j}_d$ but also to others sufficiently close in parameter space [compare Figs. 4(b) and 6(b)]. Then, noisy trajectories are composed by pieces of deterministic trajectories, some of which have collective currents. That is why the average current shown in Fig. 8 takes absolute values greater than $\bar{j}_d$

VI. CONCLUSIONS

The inclusion of defects in a system introduces different regimes of transport from those observed in a perfect lattice. While for a perfect lattice the possible currents are integers and purely collective $\bar{j} = \bar{j}_c = p$, in defective systems there appear new currents with two components, $\bar{j} = \bar{j}_c + \bar{j}_d = \pm(p + 2/s)$ (collective and defective) or only defective $\bar{j} = \bar{j}_d = \pm 2/s$.

We remark that in the thermodynamic limit ($N \to \infty, s \to \infty$, such that N/s remain finite), the current $\bar{j}_d$ vanishes. In contradistinction the collective current remains finite in this limit (since the "defective" current is just a single-particle effect).

In parameter space for a perfect lattice, there are regions that correspond to a null velocity between regions with transport in opposite directions. In the defective systems such regions correspond to purely defective currents $\pm\bar{j}_d$. That is, there is a separatrix between regions of opposite currents. When white Gaussian noise is added to a defective system lying in a parameter space region such that only defective currents are possible, then an inversion of the current may occur.

We finally remark again that our considerations made for a system with an additional particle in the perfect lattice (self-interstitial) also apply to the system with a single particle less [i.e., $N = (sl) - 1$, vacancy] with obvious variations.

ACKNOWLEDGMENTS

This work was partially supported by PICTO 00066/08 (ANPCyT) and PIP 00365/11 (CONICET–Argentina). The authors are indebted to Prof. M. A. Virasoro for fruitful discussions.

APPENDIX

The equation of motion is

$$m\ddot{x}_i(t) + \eta\dot{x}_i(t) + \frac{V_o}{d} f(s/d) + k[(x_i - x_{i-1}) + (x_i - x_{i+1})] = \frac{\epsilon}{d} g(x/d,\omega t) + \sqrt{2\eta k_B T}\,\xi_i(t), \quad \text{(A1)}$$

where $f(s/d)$ represents the dependence on the coordinates of the ratchet force, $g(x/d,\omega t)$ represents the dependence on the coordinates and the time of driving force, and $\langle \xi_i(t)\xi_i(t')\rangle = \delta(t - t')$. This equation depends on seven parameters: mass (m), damping coefficient (η), the depth of ratchet potential $2V_o$, the linear distance between consecutive minima of the ratchet potential (d), the amplitude of driving force (ϵ), the period of the driving force ($\tau = 2\pi/\omega$), the elastic constant (k), and the magnitude of the white noise ($\sqrt{2\eta k_B T}$). There are three independent dimensions: longitude, time, and energy. We take d as the unit of longitude, τ the unit of time, and $2V_o$ the unit of energy. In such way we define five adimensional parameters as

$$\Pi_m = \frac{md^2}{2V_o\tau^2}, \quad \text{(A2)}$$

$$\Pi_\eta = \frac{\eta d^2}{2V_o\tau}, \quad \text{(A3)}$$

$$\Pi_\epsilon = \frac{\epsilon}{2V_o}, \quad \text{(A4)}$$

$$\Pi_k = \frac{kd^2s^2}{2V_oN^2}, \quad \text{(A5)}$$

$$\Pi_T = \frac{k_BT}{2V_o}, \quad \text{(A6)}$$

and by replacing the parameters in Eq. (A2) we obtain

$$\Pi_m\ddot{x}_i(t) + \Pi_\eta\dot{x}_i(t) + (1/2)f(x) + \Pi_k(N/s)^2[(x_i - x_{i-1}) + (x_i - x_{i+1})] = \Pi_\epsilon g(x,t) + \sqrt{2}\sqrt{\Pi_\eta}\sqrt{\Pi_T}\,\xi_i(t), \quad \text{(A7)}$$

where the positions are measured in units of d and the time is measured in units of τ. For overdamped dynamics $\Pi_m \lll \Pi_\eta$, that is $m \lll \eta\tau$, we neglect the inertial term. In the present work we fix $\Pi_\eta = 1$, assuming overdamped dynamics.

[1] Hänggi and R. Bartussek, in *Nonlinear Physics and Complex Systems-Current Status and Future Trends*, edited by J. Parisi *et al.*, Lecture Notes in Physics (Springer, Berlin, 1996), Vol. 476, pp. 294–308.

[2] P. Reimann, Phys. Rep. **361**, 57 (2002).

[3] U. E. Vincent, A. Kenfack, D. V. Senthilkumar, D. Mayer, and J. Kurths, Phys. Rev. E **82**, 046208 (2010).

[4] A. J. Fendrik, L. Romanelli, and R. P. J. Perazzo, Physica A **359**, 75 (2006).

[5] M. F. Carusela, A. J. Fendrik, and L. Romanelli, Physica A **388**, 4017 (2009).

[6] U. E. Vincent, O. I. Olusola, D. Mayer, and P. V. E. McClintock, J. Phys. A: Math. Theor. **43**, 5101 (2010).

[7] M. von Smoluchowski, Phys. Z. **13**, 1069 (1912).

[8] R. P. Feynman, R. B. Leighton, and M. Sands, *The Feynman Lectures in Physics* (Addison-Wesley, Reading, MA, 1963).
[9] J. M. Parrondo and B. Jimenez de Cisneros, Appl. Phys. A: Mater. Sci. Process **75**, 179 (2002).
[10] R. D. Astumian and M. Bier, Phys. Rev. Lett. **72**, 1766 (1994).
[11] G. Oster and H. Wang, Trends Cell Biol. **13**, 114 (2003).
[12] J. L. Mateos, Physica A **351**, 79 (2005).
[13] M. T. Downton, M. J. Zuckermann, E. M. Craig, M. Plischke, and H. Linke, Phys. Rev. E **73**, 011909 (2006).
[14] P. Hänggi and F. Marchesoni, Rev. Mod. Phys. **81**, 387 (2010).
[15] A. J. Fendrik, L. Romanelli, and R. P. J. Perazzo, Physica A **368**, 7 (2006).
[16] F. Marchesoni, Phys. Rev. E **56**, 2492 (1997).
[17] J. J. Mazo, F. Falo, and L. M. Floría, Phys. Rev. B **52**, 6451 (1995).
[18] Y. I. Frenkel and T. Kontorova, Zh. Eksp. Theor. Fiz. **8**, 1340 (1938).
[19] A. V. Ustinov, M. Cirillo and B. A. Malomed, Phys. Rev. B **47**, 8357 (1993).
[20] T. Strunz and F.-J. Elmer, Phys. Rev. E **58**, 1601 (1998).
[21] H. Yoshino, T. Novawa, and B. Kim, Prog. Theor. Phys. Suppl. **184**, 153 (2010).
[22] V. M. Karpan, Y. Zolotaryuk, P. L. Christiansen, and A. V. Zolotaryuk, Phys. Rev. E **70**, 056602 (2004).
[23] R. DeLeo and S. Demelio, Comm. Appl. Ind. Math., doi:10.1687/journal caim.366 (2011).
[24] O. M. Braun and Y. S. Kivshar, *The Frenkel-Kontorova Model, Concepts, Methods and Applications* (Springer-Verlag, Berlin-Heidelberg, 2004).
[25] Z. Csahók, F. Family, and T. Vicsek, Phys. Rev. E **55**, 5179 (1997).
[26] L. M. Floría, F. Falo, P. J. Martínez, and J. J. Mazo, Europhys. Lett. **60**, 174 (2002).
[27] L. M. Floría, C. Baesens, and J. Gómez-Gardeñes, Lectures Notes in Physics **671**, 209 (2005).
[28] A. J. Fendrik, M. Reale, and L. Romanelli, Physica A **390**, 3932 (2011).